Mini-Curso
Fabricação e Caracterização de Nanoestruturas

CBPF - Rio de Janeiro, 20-24 Março, 2006

Unidade 2: Técnicas de Microscopia Eletrônica de Transmissão

Aula 2 – Difração de Elétrons

Por:

Antônio J. Ramirez
Laboratório Nacional de Luz Síncrotron

LNLS
2006/2-1

Conteúdo

- Introdução
  - Definições
- Ótica Eletrônica
  - Fontes de elétrons
  - Lentes magnéticas
  - Aberrações
- Interação Elétron Matéria
  - Sinais
  - Dano na amostra
- Microscopia Eletrônica de Transmissão (TEM)
  - Configuração do equipamento
  - Microscopia de transmissão por varredura
  - Difração de elétrons
  - Tipos de imagem
  - Técnicas de microscopia convencional
  - Aplicações
  - Preparação de Amostras
  - Microscopia de alta resolução – contraste de fase
- Espectroscopia de Raios –X Dispersiva em Energia (EDS)
- Espectroscopia de Elétrons (EELS)

LNLS
2006/2-2

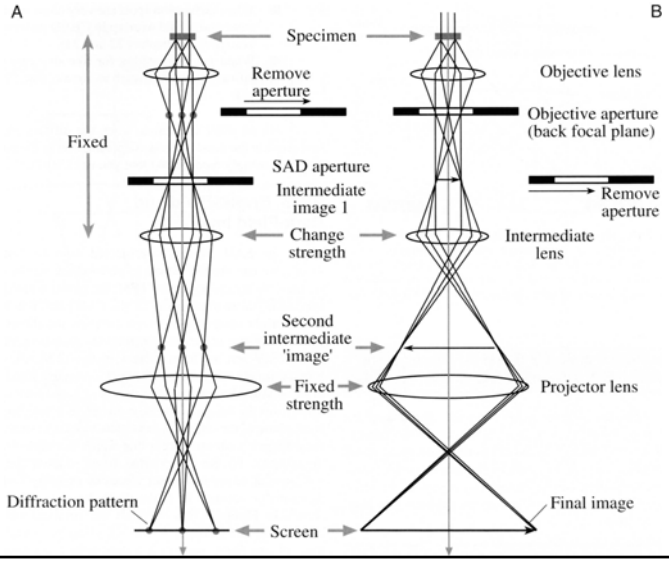
Referencias

TEM-EELS

- D.B. Williams, C.B. Carter, Transmission Electron Microscopy, Plenum Press, New York, 1996.
- L. Remier, Transmission Electron Microscopy, 4th Ed., Springer-Verlag, New York, 1997.
- J.W. Edington, Practical Electron Microscopy in Materials Science, N.V. Philips, Eindhoven, 1976.

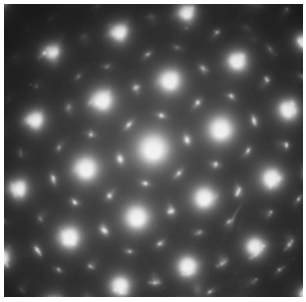
2006/2-3

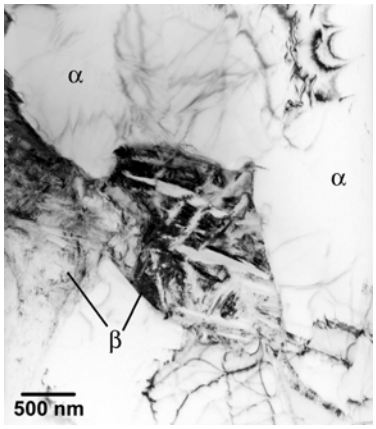
Formação de Imagem



2006/2-4

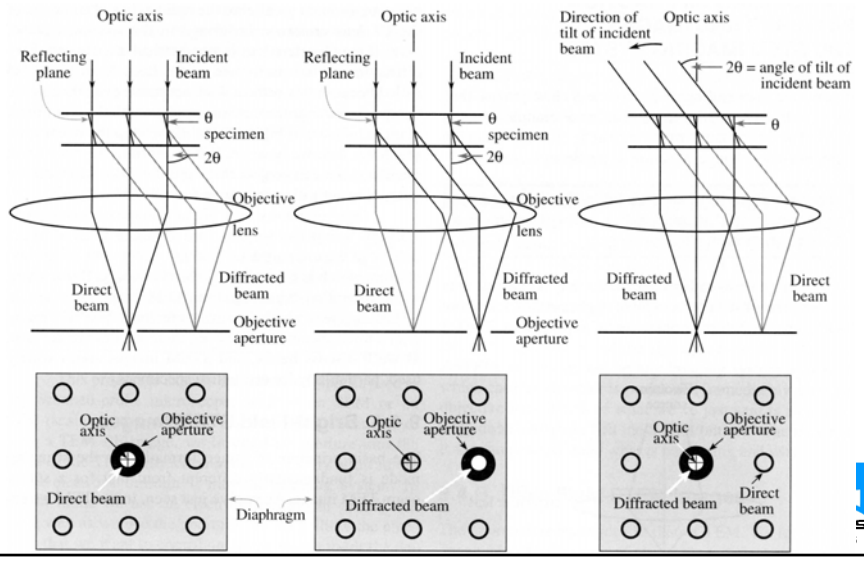
Modos de Imagem e Difração - TEM



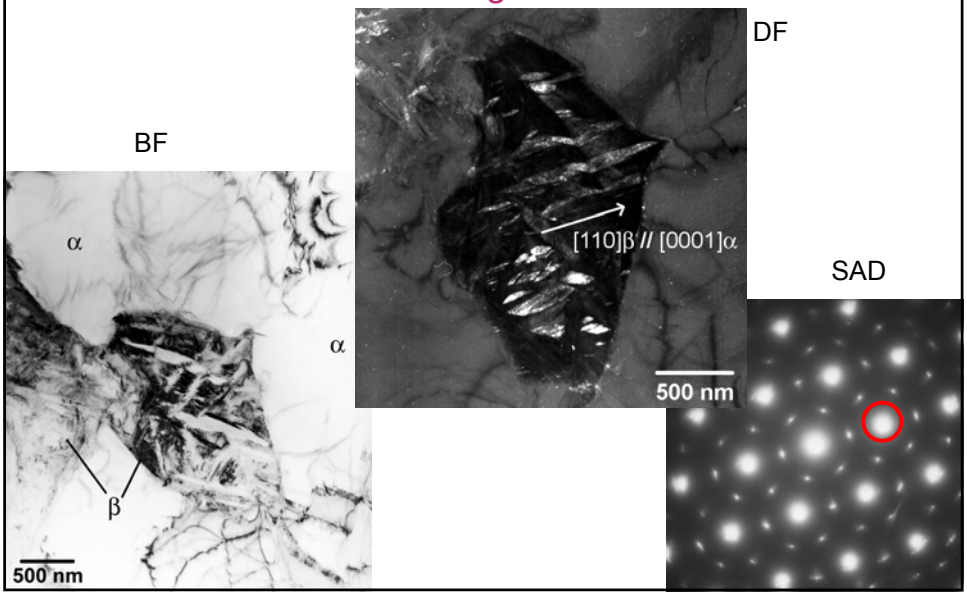


2006/2-5

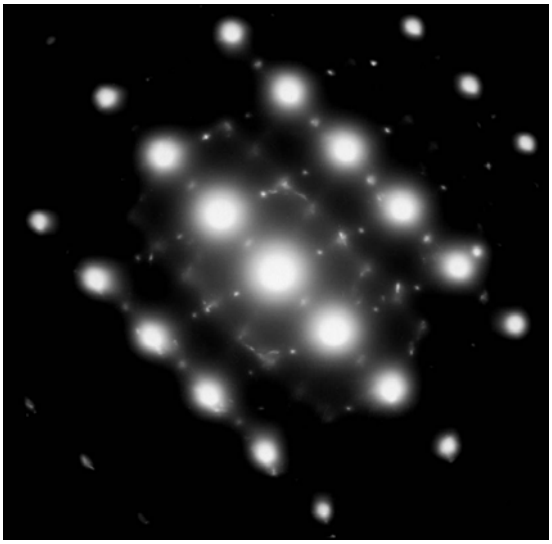
Modos de Imagem em TEM



Modos de Imagem em TEM

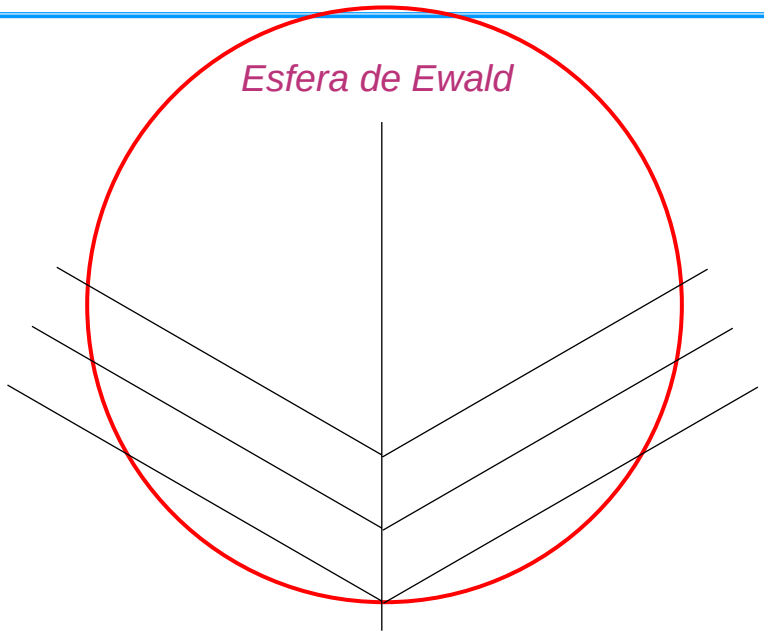


Difração de Elétrons



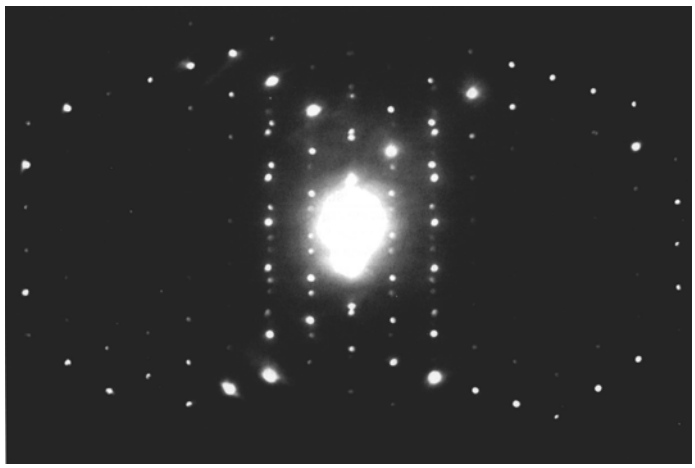
LNLS
2006/2-8

Esfera de Ewald



LNLS
2006/2-9

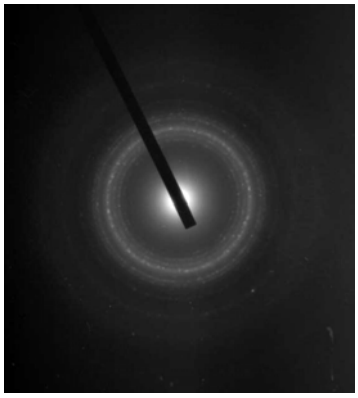
Interface de Macla



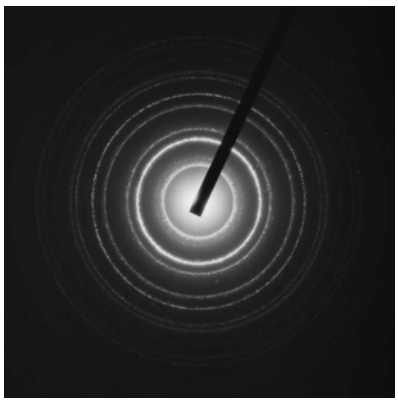
LNLS
2006/2-10

Difração

Co



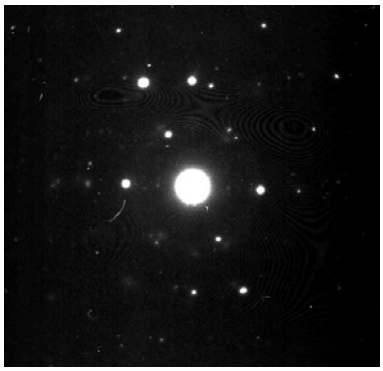
Ag



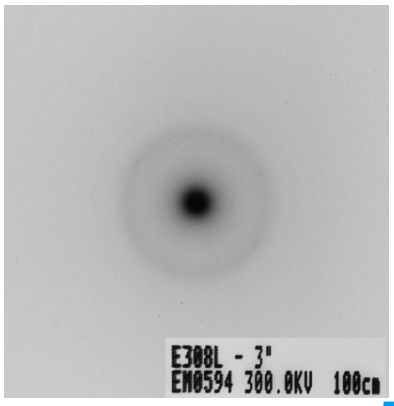
LNLS
2006/2-11

Difração

Cristalino

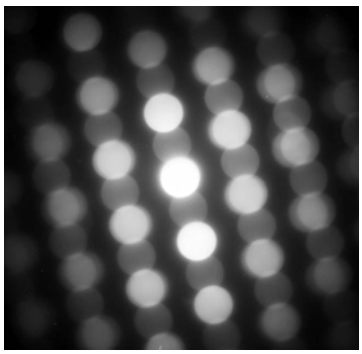


Amorfo

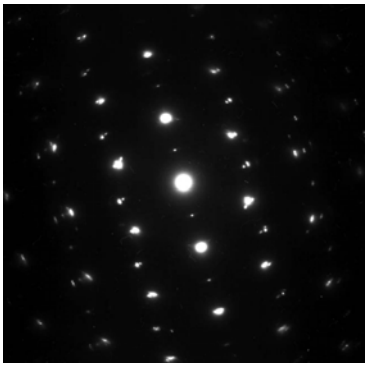


LNLS
2006/2-13

Difração



Convergent Beam

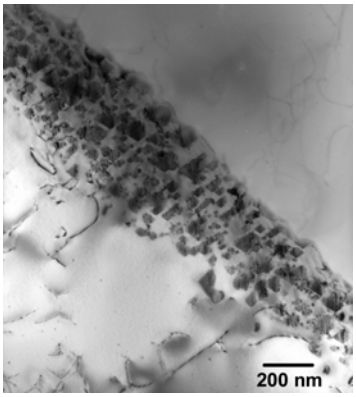


Parallel Beam

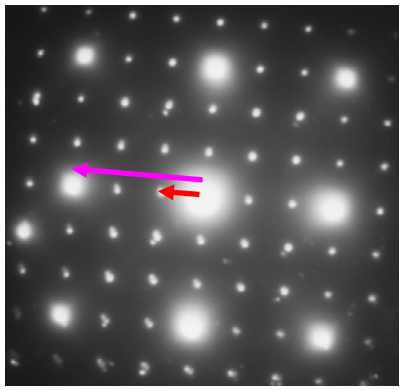
2006/2-14

Microscopia Eletrônica de Transmissão Antônio J. Ramirez

Difração – Relação de Orientação



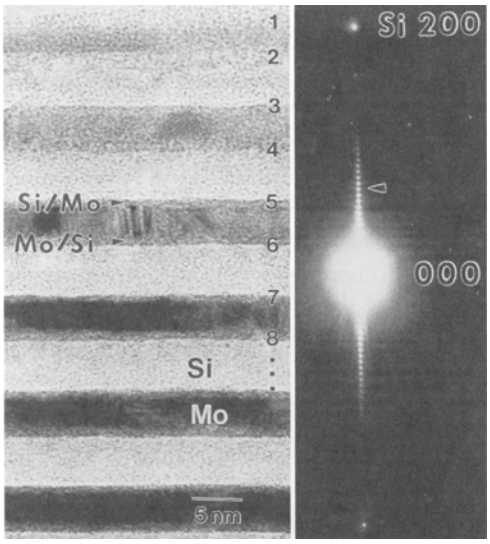
$M_{23}C_6$ FCC
Austenite FCC



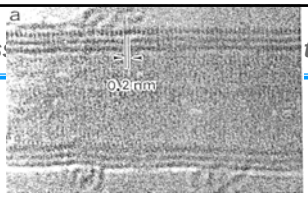
[001] // [001], (200) // (200)

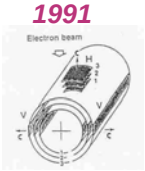
2006/2-15

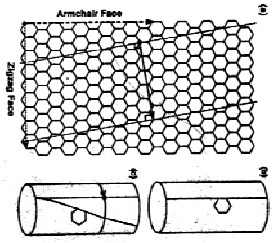
Super-Reticulado

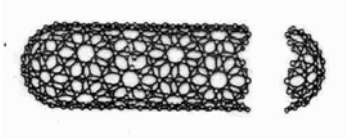


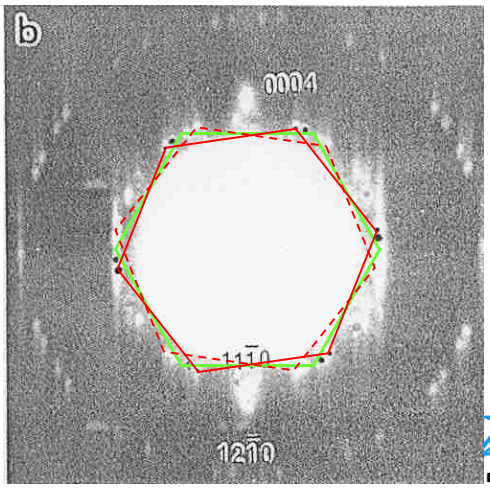
2006/2-16





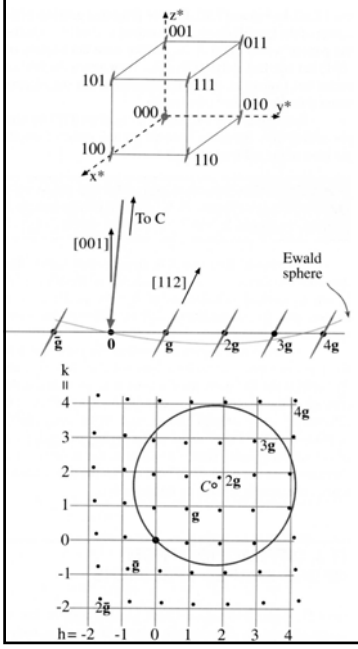






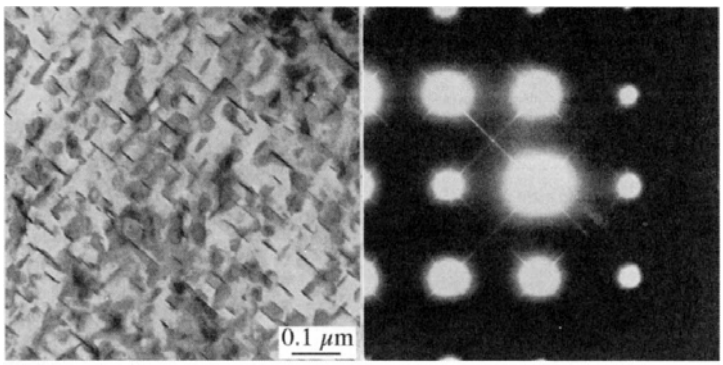
2006/2-17

Efeito da Lámina Fina



2006/2-18

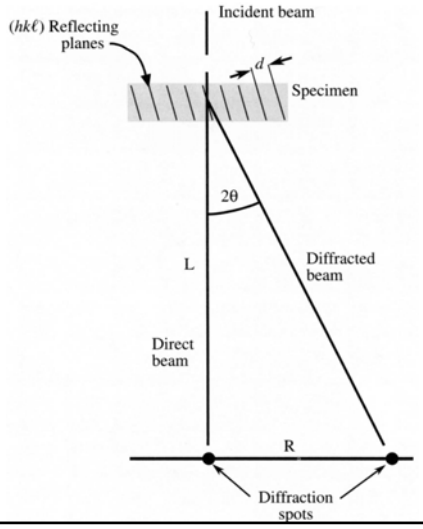
Difração de Pequenos Volumes



Very thin plate-like precipitates (A) cause long streaks in the DP (B). In this example, the precipitates are GP zones in an Fe-2.9 at % Mo alloy.

2006/2-19

Constante de Câmera



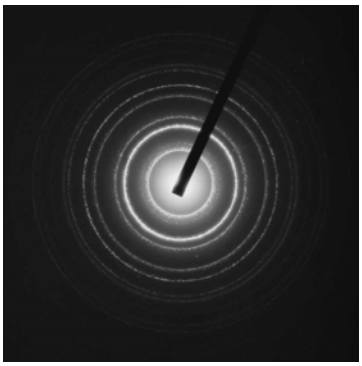
$$\tan 2\theta = \frac{R}{L} \sim 2\theta$$

$$\frac{\lambda}{d} = 2\,\mathrm{sen}\,\theta \sim 2\theta$$

$$Rd = \lambda L[\text{mm Å}]$$

2006/2-22

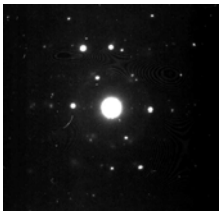
Constante de Câmera



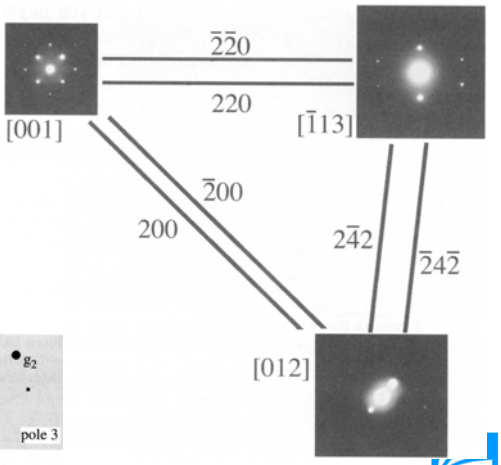
Ag

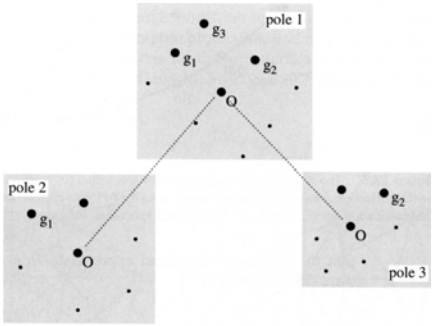
dÅ	i-f	h	k	l
2.3590	100	1	1	1
2.0440	40	2	0	0
1.4450	25	2	2	0
1.2310	26	3	1	1
1.1796	12	2	2	2
1.0215	4	4	0	0
.93750	15	3	3	1
.91370	12	4	2	0
.83410	13	4	2	2

2006/2-23

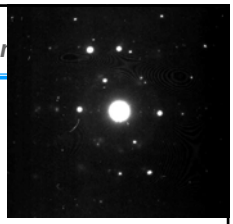


Indexação (Trabalho no TEM)





LNLS
2006/2-24

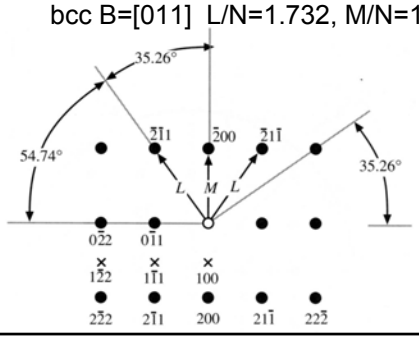


Indexação

$$Rd = \lambda L \qquad R_1 d_1 = R_2 d_2 = R_3 d_3 = R_4 d_4 = \cdots$$

$$\cos(\phi_{AB}) = \frac{\mathbf{g}_A \cdot \mathbf{g}_B}{|\mathbf{g}_A||\mathbf{g}_B|}$$

bcc B=[011] L/N=1.732, M/N=1.414



LNLS
2006/2-25

Microscopia Eletrônica de Transmissão — Antônio J. Ramirez

Indexação

$$\cos(\phi_{AB}) = \frac{\mathbf{g}_A \cdot \mathbf{g}_B}{|\mathbf{g}_A||\mathbf{g}_B|}$$

$$\cos\phi = \frac{h_1h_2 + k_1k_2 + \ell_1\ell_2}{\left(h_1^2 + k_1^2 + \ell_1^2\right)^{\frac{1}{2}}\left(h_2^2 + k_2^2 + \ell_2^2\right)^{\frac{1}{2}}}$$

$$\cos\rho = \frac{U_1U_2 + V_1V_2 + W_1W_2}{\left(U_1^2 + V_1^2 + W_1^2\right)^{\frac{1}{2}}\left(U_2^2 + V_2^2 + W_2^2\right)^{\frac{1}{2}}}$$

$$\mathbf{B} = \mathbf{g}_1 \times \mathbf{g}_2 = \begin{bmatrix} \mathbf{i}_1 & \mathbf{i}_2 & \mathbf{i}_3 \\ h_1 & k_1 & \ell_1 \\ h_2 & k_2 & \ell_2 \end{bmatrix}$$

$$= (k_1\ell_2 - k_2\ell_1,\ \ell_1h_2 - \ell_2h_1,\ h_1k_2 - h_2k_1)$$

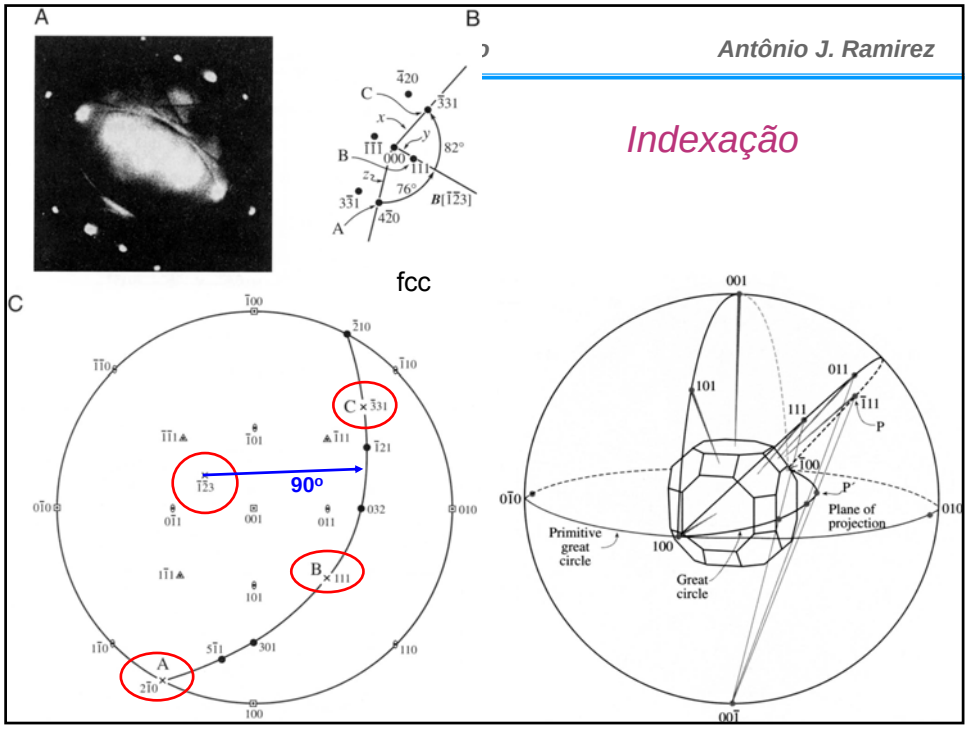
$$\mathbf{B} = \frac{\mathbf{g}_2 \times \mathbf{g}_3}{|\mathbf{g}_1|^2} + \frac{\mathbf{g}_3 \times \mathbf{g}_1}{|\mathbf{g}_2|^2} + \frac{\mathbf{g}_1 \times \mathbf{g}_3}{|\mathbf{g}_3|^2}$$

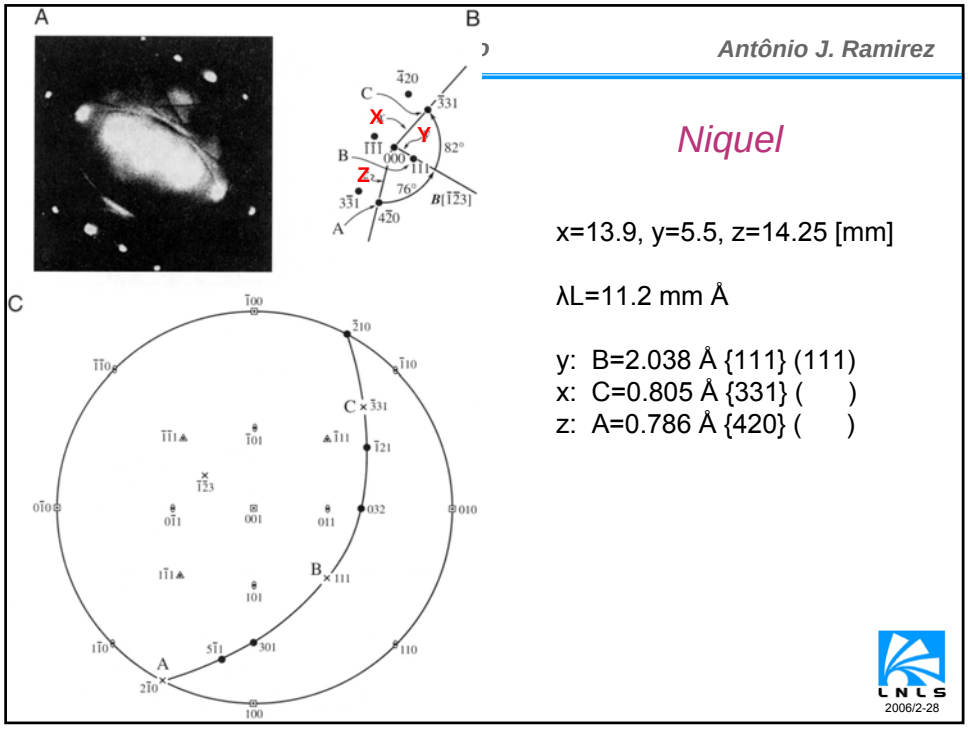
Refleções (*hkl*) num eixo de zona [*UVW*]

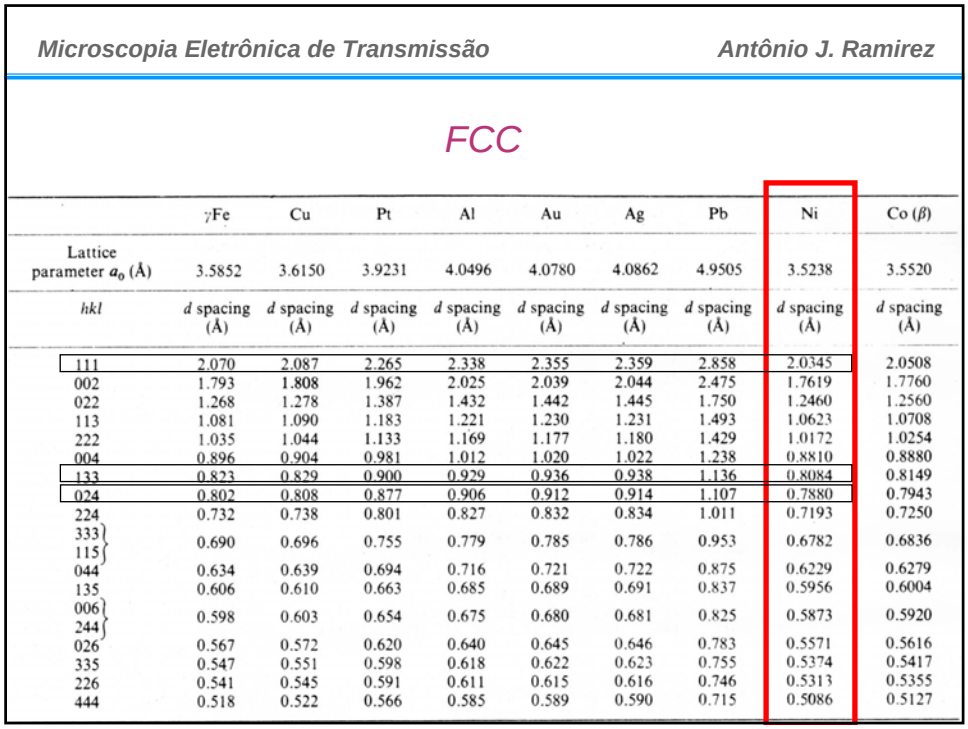
hU+kV+lW=n (n: zona de Laue)

(000) dentro: anti-horário
(000) fora : horário

2006/2-26







	γFe	Cu	Pt	Al	Au	Ag	Pb	Ni	Co (β)
Lattice parameter a_0 (Å)	3.5852	3.6150	3.9231	4.0496	4.0780	4.0862	4.9505	3.5238	3.5520
hkl	*d* spacing (Å)	*d* spacing (Å)	*d* spacing (Å)	*d* spacing (Å)	*d* spacing (Å)	*d* spacing (Å)	*d* spacing (Å)	*d* spacing (Å)	*d* spacing (Å)
111	2.070	2.087	2.265	2.338	2.355	2.359	2.858	2.0345	2.0508
002	1.793	1.808	1.962	2.025	2.039	2.044	2.475	1.7619	1.7760
022	1.268	1.278	1.387	1.432	1.442	1.445	1.750	1.2460	1.2560
113	1.081	1.090	1.183	1.221	1.230	1.231	1.493	1.0623	1.0708
222	1.035	1.044	1.133	1.169	1.177	1.180	1.429	1.0172	1.0254
004	0.896	0.904	0.981	1.012	1.020	1.022	1.238	0.8810	0.8880
133	0.823	0.829	0.900	0.929	0.936	0.938	1.136	0.8084	0.8149
024	0.802	0.808	0.877	0.906	0.912	0.914	1.107	0.7880	0.7943
224	0.732	0.738	0.801	0.827	0.832	0.834	1.011	0.7193	0.7250
333, 115	0.690	0.696	0.755	0.779	0.785	0.786	0.953	0.6782	0.6836
044	0.634	0.639	0.694	0.716	0.721	0.722	0.875	0.6229	0.6279
135	0.606	0.610	0.663	0.685	0.689	0.691	0.837	0.5956	0.6004
006, 244	0.598	0.603	0.654	0.675	0.680	0.681	0.825	0.5873	0.5920
026	0.567	0.572	0.620	0.640	0.645	0.646	0.783	0.5571	0.5616
335	0.547	0.551	0.598	0.618	0.622	0.623	0.755	0.5374	0.5417
226	0.541	0.545	0.591	0.611	0.615	0.616	0.746	0.5313	0.5355
444	0.518	0.522	0.566	0.585	0.589	0.590	0.715	0.5086	0.5127

Difração

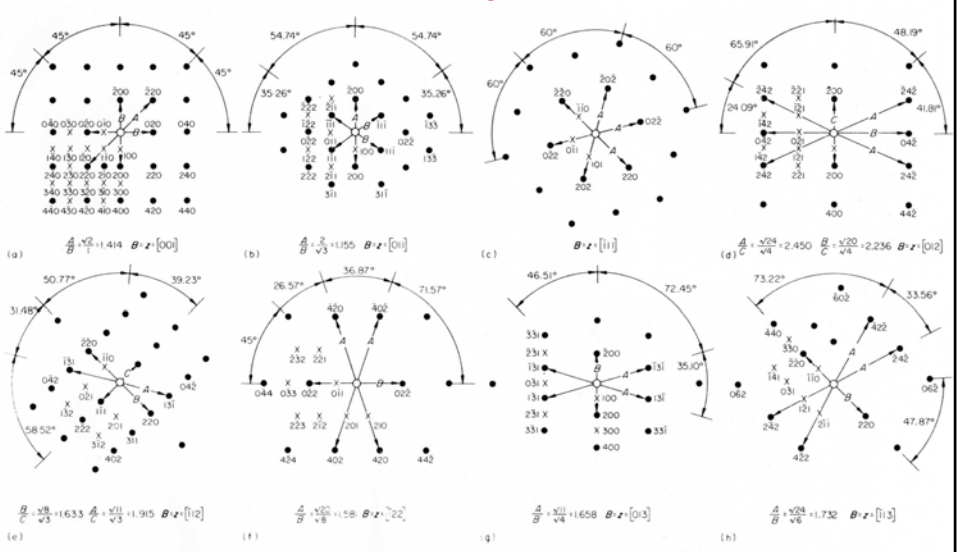
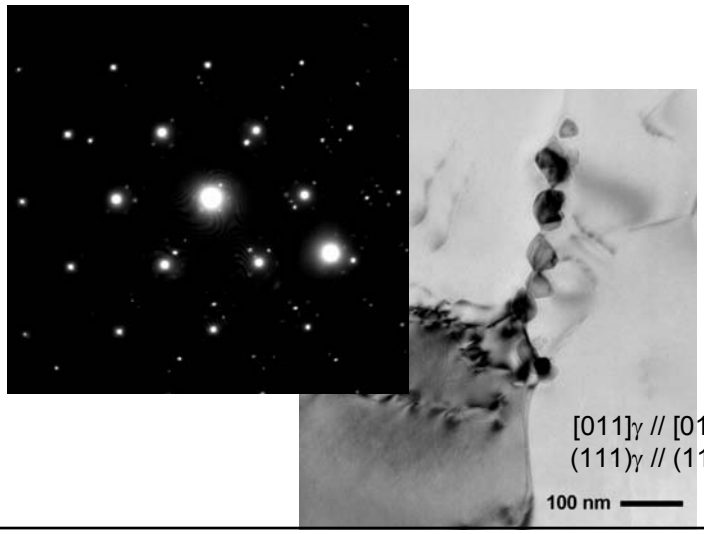


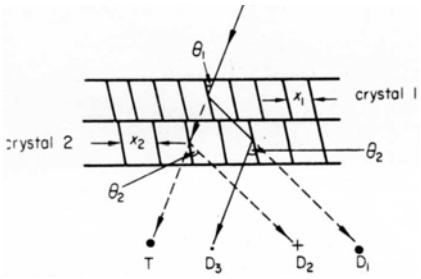
Figure A4.1 Single-crystal spot transmission electron diffraction patterns for the f.c.c. crystal structure ($u^2 + v^2 + w^2 < 22$). The zone axis z, defined in appendix 1, is the beam direction B defined in section 2.7.2, as indicated. The crosses in one quadrant of the diagram indicate the positions of the spots for the ordered f.c.c. ($L1_2$) unit cell. The complete pattern may be generated by repeating these spots in the remainder of the pattern and indexing using the addition of vectors, see section 2.7.2.1

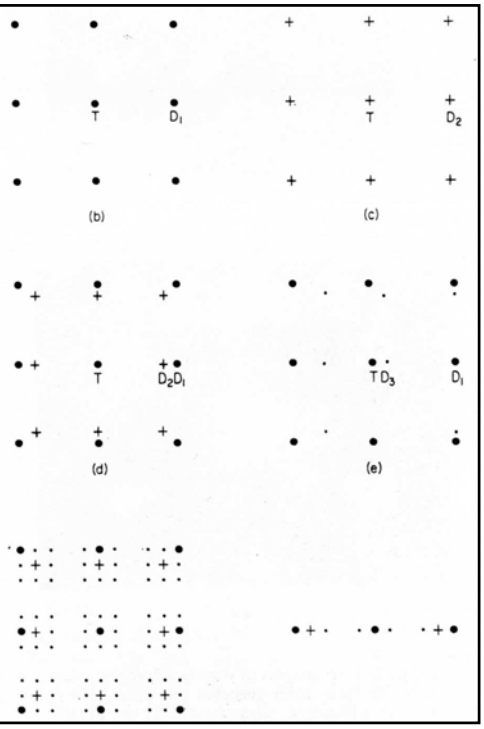
Dupla Difração



Microscopia Eletrônica de Transmissão

Dupla Difração

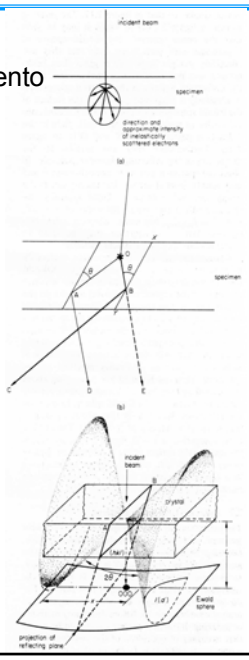


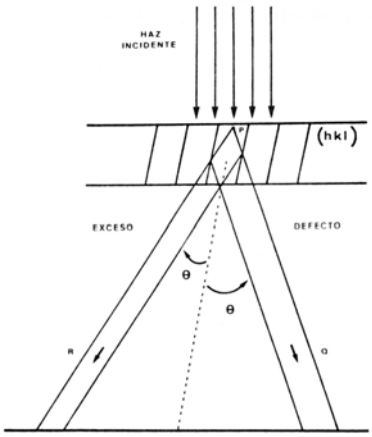


Microscopia Eletrônica de Transmissão Antônio J. Ramirez

Difração

Espalhamento Difuso

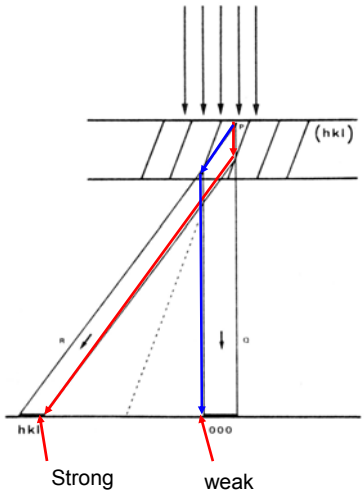


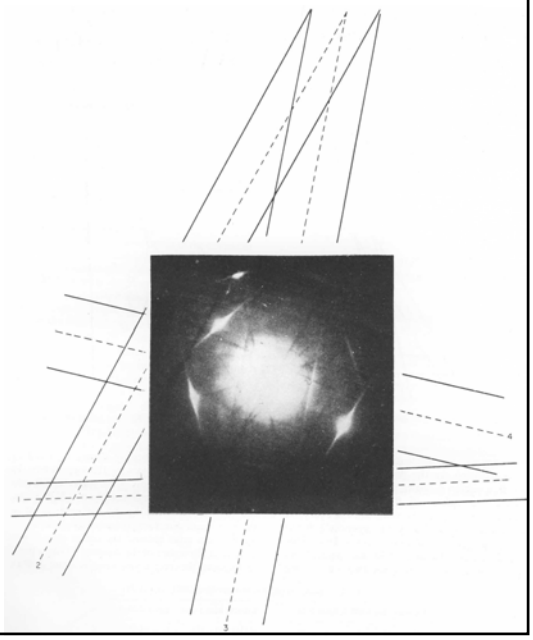


Linhas de Kikuchi

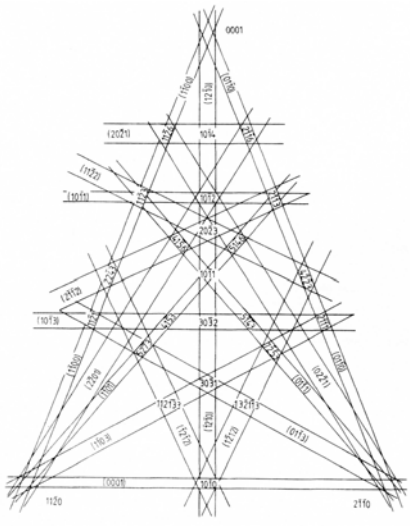
LNLS
2006/2-33

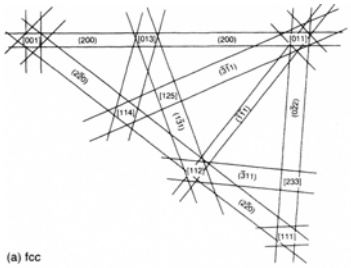
Difração





Mapas de Kikuchi





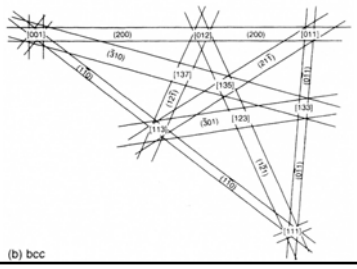
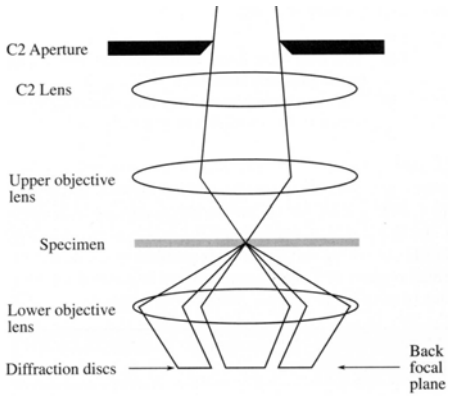
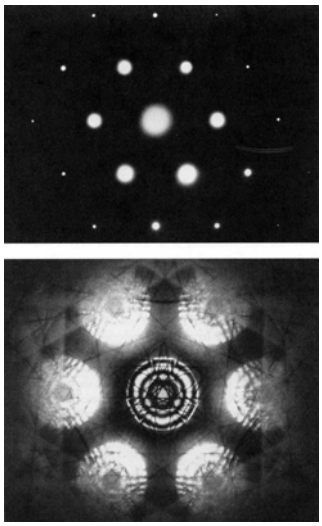


Figure A6.2 Kikuchi map for hexagonal crystal structures (Ti, $c/a \approx 1.59$, two stereographic triangles).

2006/2-35

Difração de Feixe Convergente - CBED





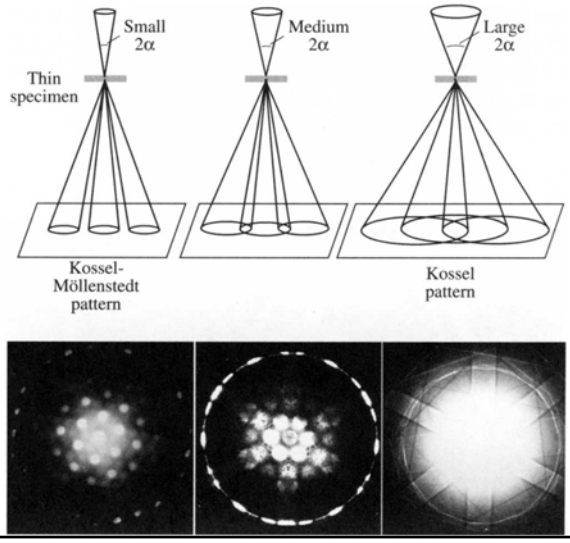
SAD

CBED

2006/2-36

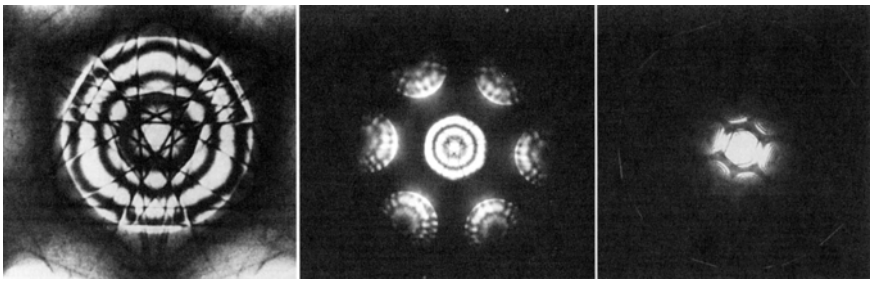
Microscopia Eletrônica de Transmissão Antônio J. Ramirez

Difração de Feixe Convergente - CBED



2006/2-37

Difração de Feixe Convergente - CBED

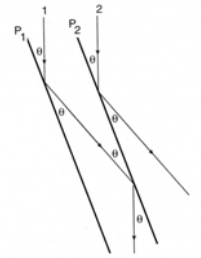


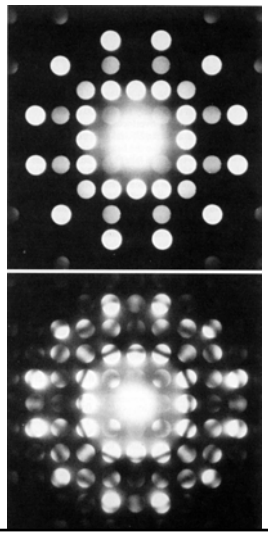
Variação de L (Magnificação)

2006/2-38

Microscopia Eletrônica de Transmissão Antônio J. Ramirez

Difração de Feixe Convergente - CBED



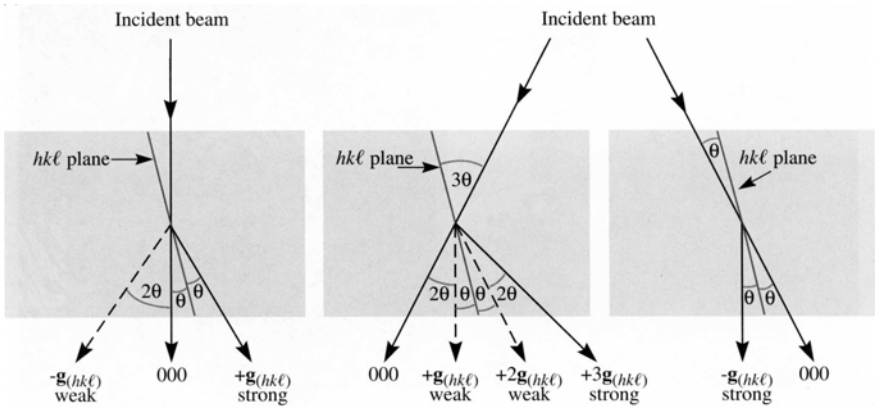


Cinemática

Dinâmica

2006/2-39

Condição de 2 Feixes – Two Beam



2006/2-40

Franjas de Espessura

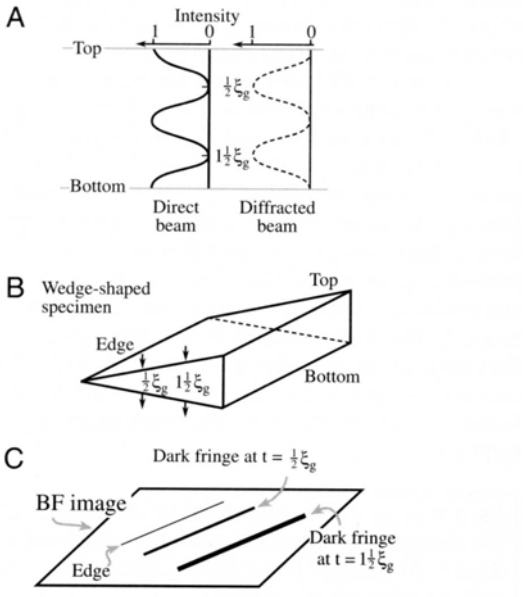


Figure 23.2. (A) At the Bragg condition (s = 0), the intensities of the direct and diffracted beams oscillate in a complementary way. (B) For a wedge specimen, the separation of the fringes in the image (C) is determined by the angle of the wedge and the extinction distance, ξ_g.

2006/2-41

Franjas de Espessura

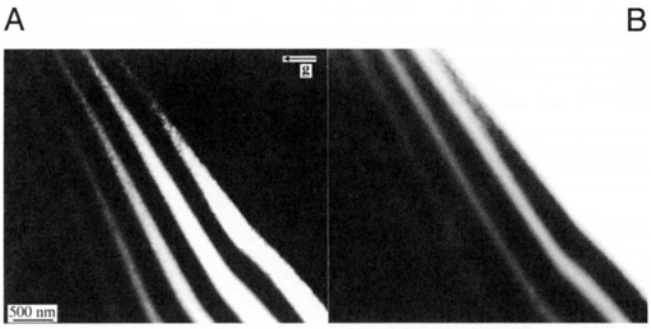
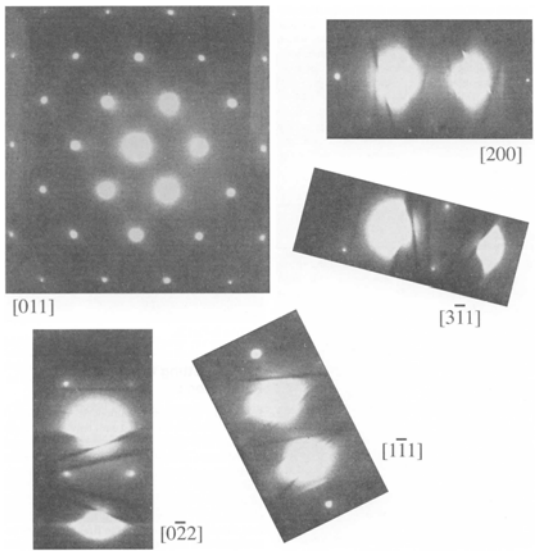
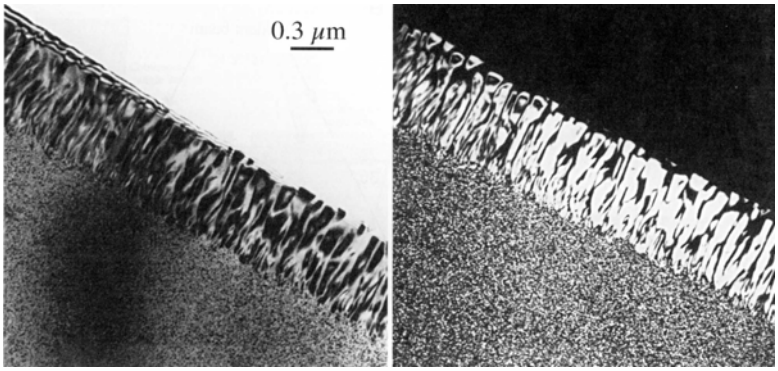


Figure 23.1. (A) DF and (B) BF images from the same region of a wedge-shaped specimen of Si at 300 kV tilted so that **g**(220) is strong. The periodicity and contrast of the fringes is similar and complementary in each image.

Condição de 2 Feixes



Condição de 2 Feixes

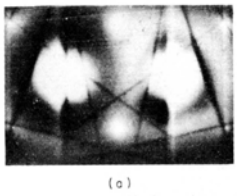


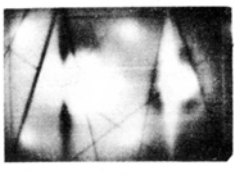
Erro de Excitação (s)

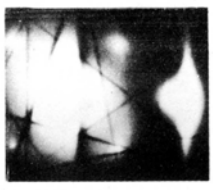


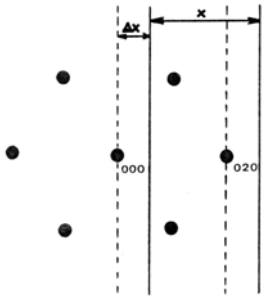
S<0

S>0



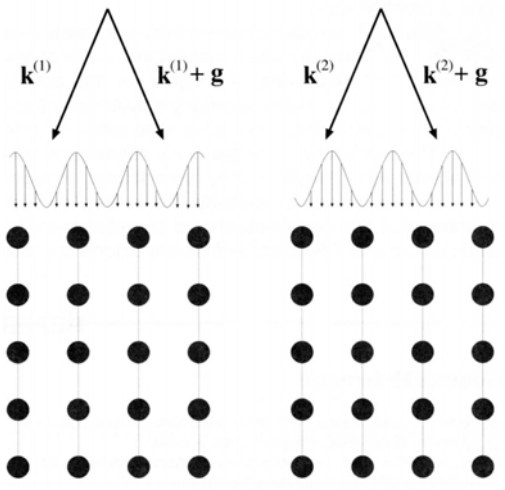






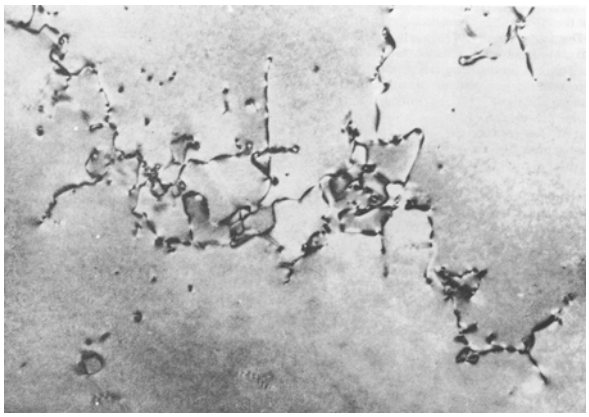
Ondas de Bloch

Predomina S<0

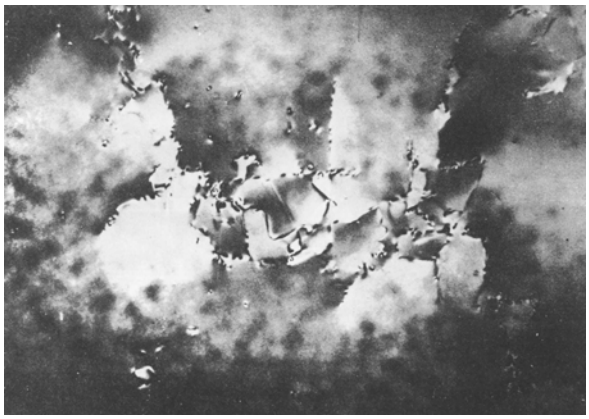


Predomina S>0

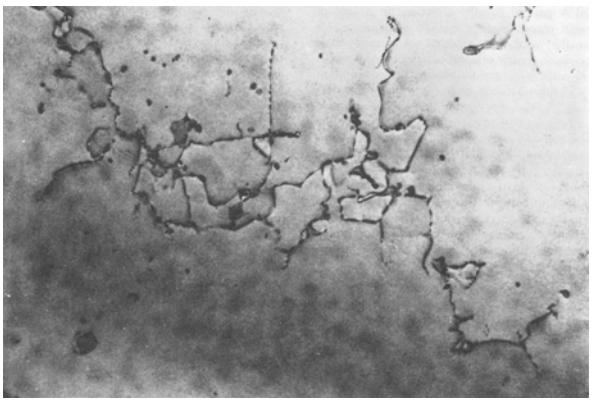
Erro de Excitação (s) = 0



Erro de Excitação (s) < 0

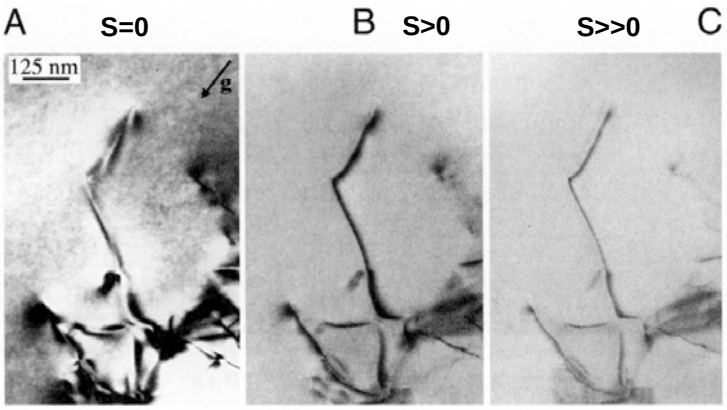


Erro de Excitação (s) > 0



Condição Ideal para Contraste

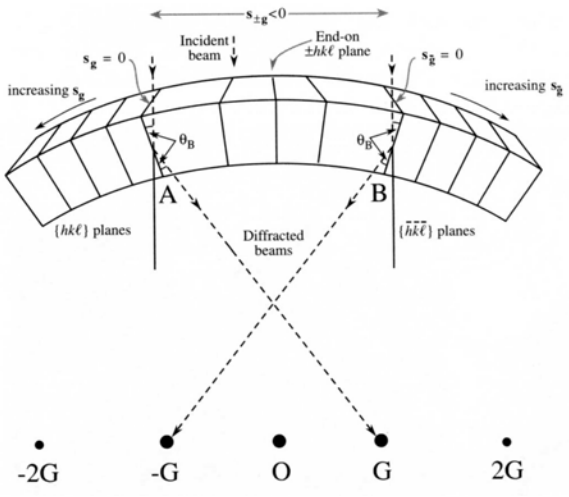
Erro de Excitação (s)



Variation in the diffraction contrast when **s** is varied from (A) zero to (B) small and positive and (C) larger and positive.

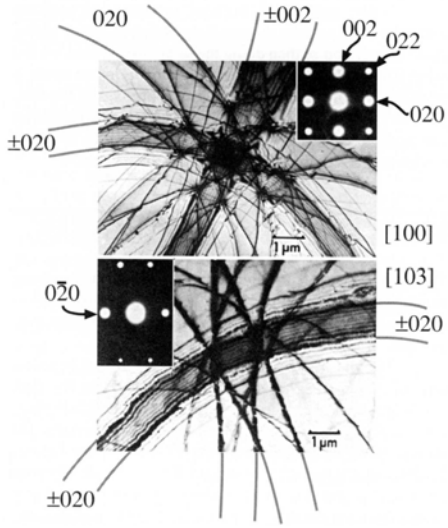
2006/2-50

Contornos de Dobramento



2006/2-51

Contornos de Dobramento



2006/2-52

Defeitos Planares

- Translation Boundary
  - Falha de Empilhamento
  - Anti-Phase Boundary
- Grain Boundary
  - Σ
- Phase Boundary
- Surface

2006/2-53

Condição de 2 Feixes – Dif. Dinâmica

Howie-Whelan eqs.

$$\frac{d\phi_g}{dz} = \frac{\pi i}{\xi_g}\phi_0 e^{-2\pi i s z} + \frac{\pi i}{\xi_0}\phi_g$$

$$\frac{d\phi_0}{dz} = \frac{\pi i}{\xi_0}\phi_0 + \frac{\pi i}{\xi_g}\phi_g e^{2\pi i s z}$$

$$\frac{d\phi_g}{dz} = \frac{\pi i}{\xi_0}\phi_g + \frac{\pi i}{\xi_g}\phi_0 \exp\left[-2\pi i\left(sz + \mathbf{g}\cdot\mathbf{R}\right)\right]$$

$$\frac{d\phi_0}{dz} = \frac{\pi i}{\xi_0}\phi_0 + \frac{\pi i}{\xi_g}\phi_g \exp\left[+2\pi i\left(sz + \mathbf{g}\cdot\mathbf{R}\right)\right]$$

LNLS 2006/2-54

Mudança de Fase Devido ao Defeito

$$\alpha = 2\pi \mathbf{g}\cdot\mathbf{R}$$

O defeito planar causa contraste quando α é diferente de zero

$\alpha = 120^o$ em SFs de FCC

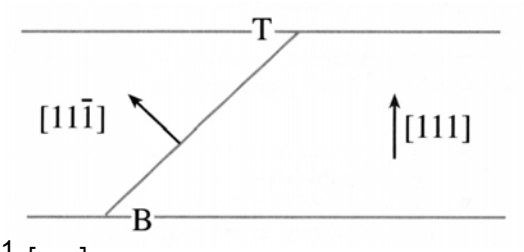
- A imagem depende da espessura
- Imagens campo obscuro e claro não são complementarias como no caso de franjas de espessura

LNLS 2006/2-55

SF in FCC Materials

$$R = \frac{1}{6}\langle \bar{1}\,\bar{1}\,2\rangle$$

$$R = \frac{1}{3}\langle 111\rangle$$



$$R = \pm\frac{1}{3}[11\bar{1}]$$

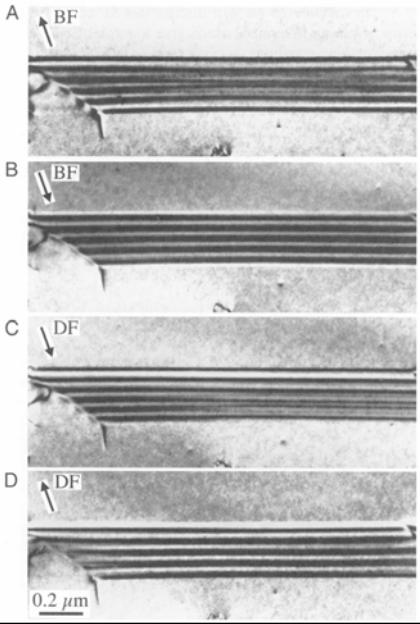
$$g = (2\bar{2}0) \rightarrow g.R = 0$$

$$g = (02\bar{2}) \rightarrow g.R = \pm\frac{4}{3} \rightarrow \alpha = \frac{8\pi}{3} = \frac{2\pi}{3} = 120^{\circ}$$

$$\alpha = -\frac{8\pi}{3} = -\frac{2\pi}{3} = -120^{\circ}$$

LNLS 2006/2-56

SF in FCC



LNLS 2006/2-57

Contrast Modulation on Planar Defects

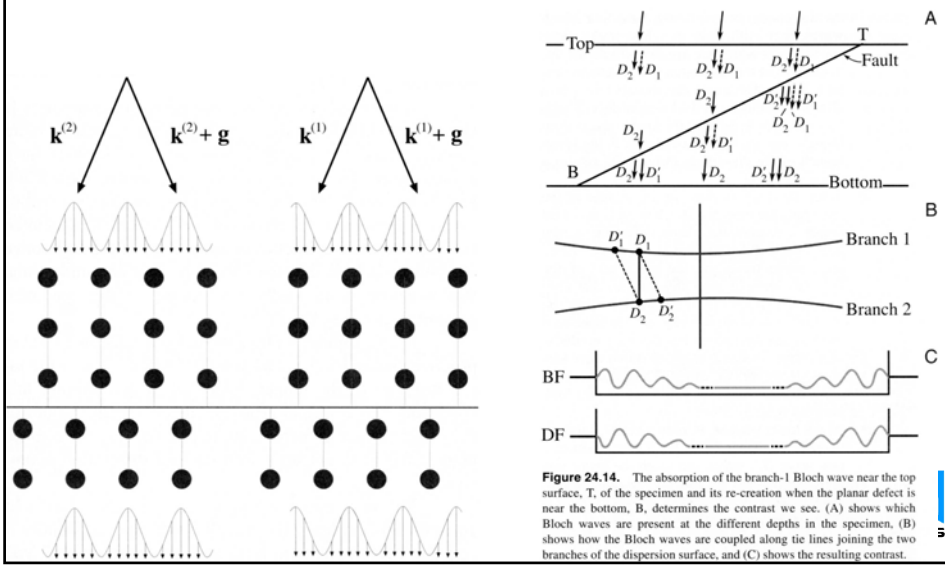
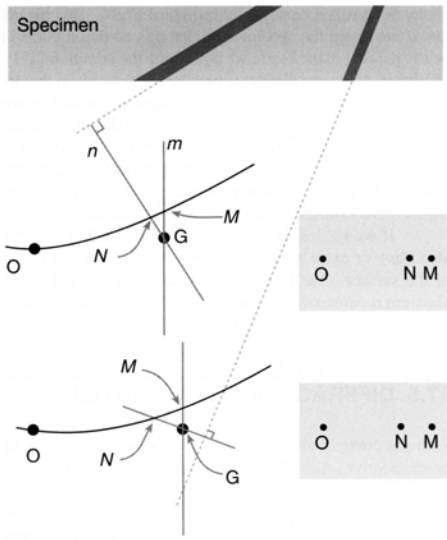


Figure 24.14. The absorption of the branch-1 Bloch wave near the top surface, T, of the specimen and its re-creation when the planar defect is near the bottom, B, determines the contrast we see. (A) shows which Bloch waves are present at the different depths in the specimen, (B) shows how the Bloch waves are coupled along tie lines joining the two branches of the dispersion surface, and (C) shows the resulting contrast.

Defeito Planar - Difração



2006/2-59

Deslocamento-Deformação-Tensão

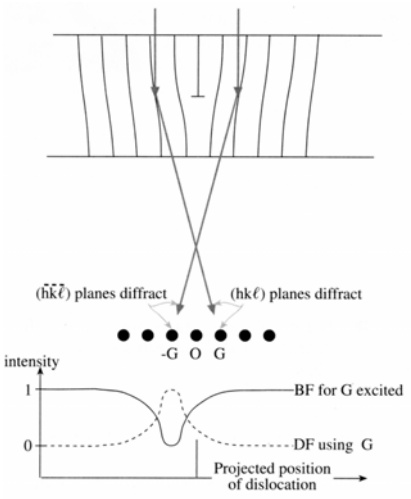
- R(r) : Campo de Deslocamento
- ε(r) : Campo de Deformação
- σ(r) : Campo de Tensão

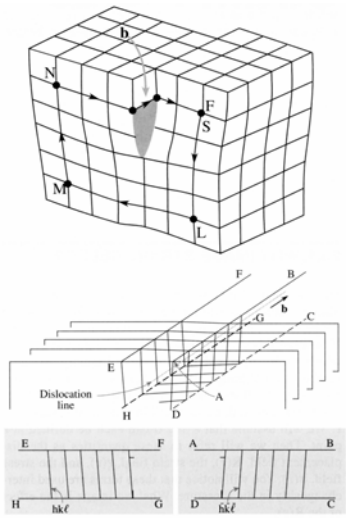
O deslocamento gera contraste no TEM

Discordâncias - Dislocações

- Direção e magnitude do vetor de Burgers (**b**) $\perp$ plano hkl em condição de difração
- Linha (Vetor), define cunha, parafuso, mista
- Plano de escorregamento
- Interação com outras discordâncias
- Curvada, hélice
- Densidade

Discordâncias





2006/2-62

Efeito do S no Contraste

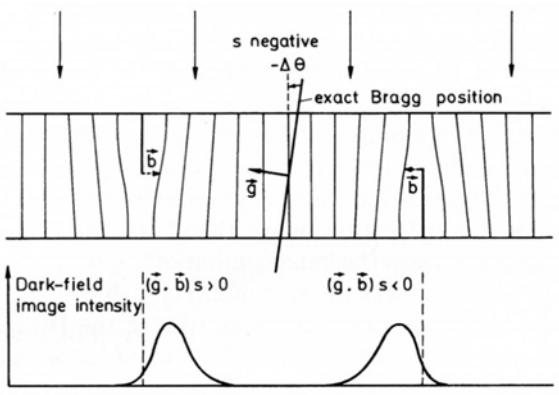
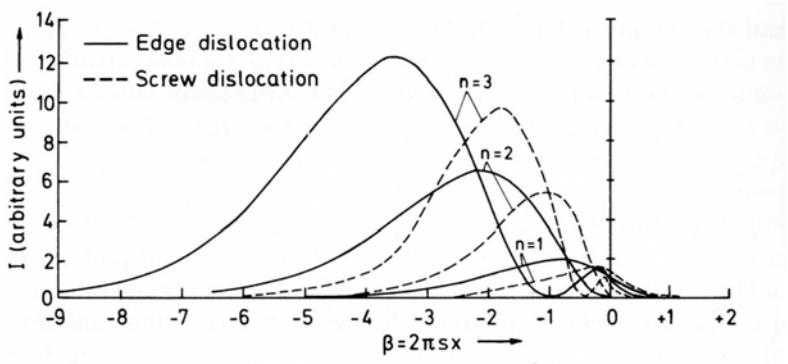


Fig. 9.21. Diagram showing on which side of its core the dislocation image is situated

2006/2-63

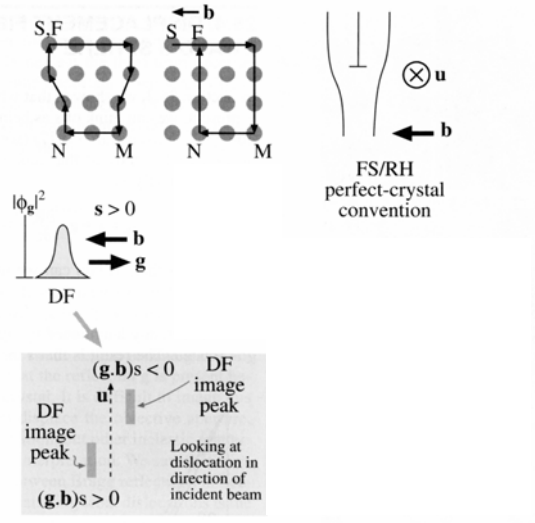
Perfil de Intensidade



Intensity profiles proportional to $\overline{AB}^2$ in Fig. 9.19 across the dark-field images of edge and screw dislocations with different values of $\boldsymbol{g} \cdot \boldsymbol{b} = n$. The centre of the dislocation is at $x = 0$ [9.50]

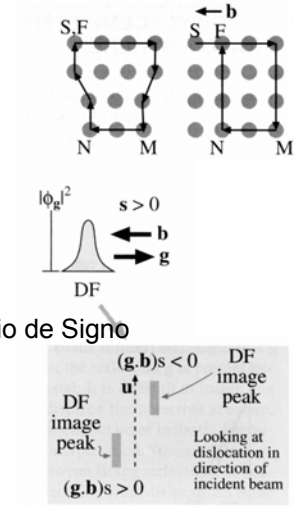
2006/2-64

Discordâncias - FCC



2006/2-65

Discordâncias



Cambio de Signo

Imagem com s>0 (Dislocation is black)

g.b=0 Sem contraste (R ll planos difratam)

g_1.b=g_2.b=0 → g_1xg_2 ll b

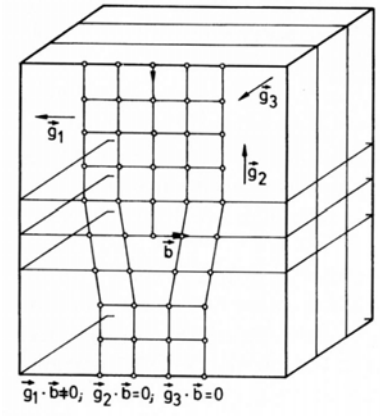
Problema devido a:

falta de contraste para g.b<1/3

Contraste para **g.b=0** onde **g.bxu ≠0**

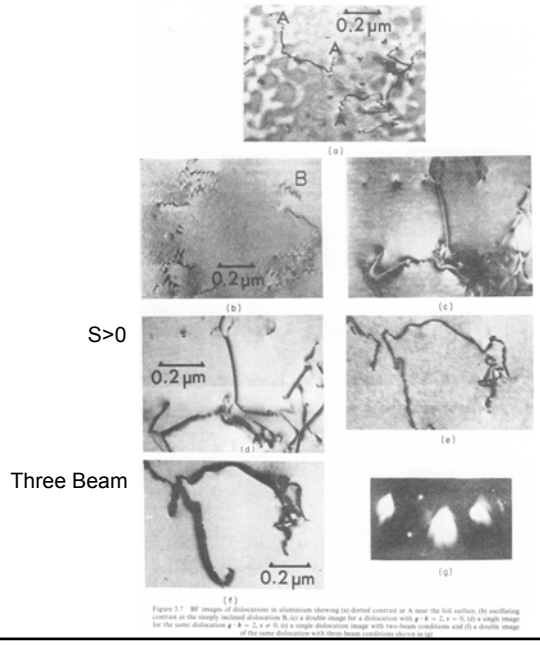
2006/2-68

g.b = 0



Demonstration of the $\boldsymbol{g} \cdot \boldsymbol{b} = 0$ rule for an edge dislocation. Only the lattice planes that belong to $\boldsymbol{g}_1$ are strongly bent, so that $\boldsymbol{g}_1 \cdot \boldsymbol{b} \neq 0$ whereas $\boldsymbol{g}_2 \cdot \boldsymbol{b} = \boldsymbol{g}_3 \cdot \boldsymbol{b} = 0$

2006/2-69



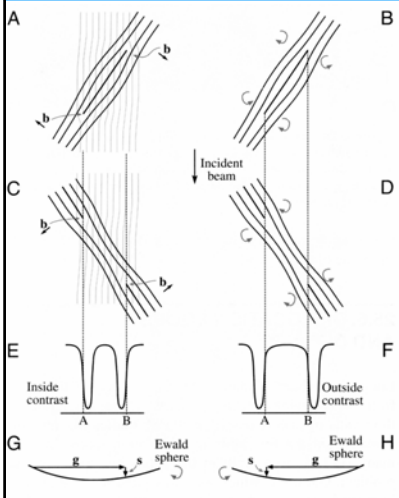


Figure 25.9. (A) Structure of an interstitial loop relative to the diffracting planes (faint lines). (B) Arrows show the rotation of the diffracting planes around the dislocation. (C,D) Vacancy loops. (E,F) Position of the image contrast relative to the projected dislocation position. Inside contrast occurs when clockwise rotation of the diffracting planes brings them into the Bragg condition. Outside contrast occurs for the counterclockwise case. (G,H) The relationship between **g**, **s** and the sense of rotation. Everything is reversed if the loops are tilted in the opposite direction relative to the beam (i.e., reflect this figure in a mirror).

Discordâncias - Loops

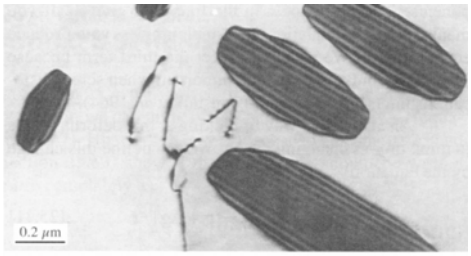


Figure 25.10. Dislocation loops in irradiated Ni showing SF contrast.

Emaranhados de Discordâncias

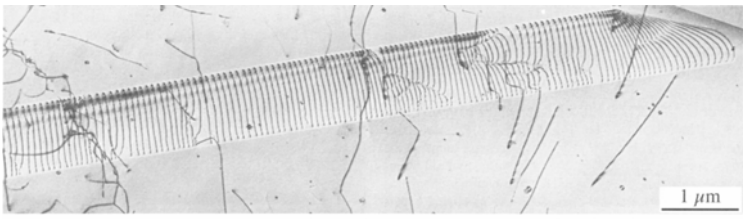
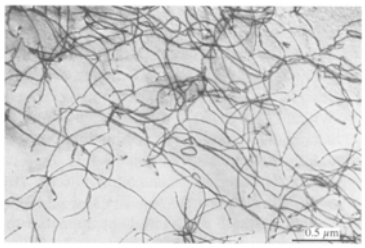


Figure 25.14. Dislocations threading through a very thick specimen in an image recorded using a high-voltage TEM.



LNLS
2006/2-74

Partículas Esféricas

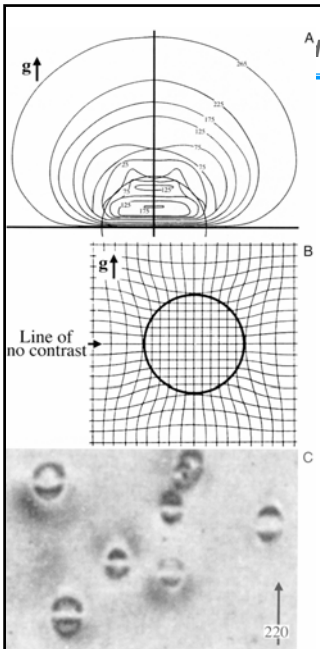
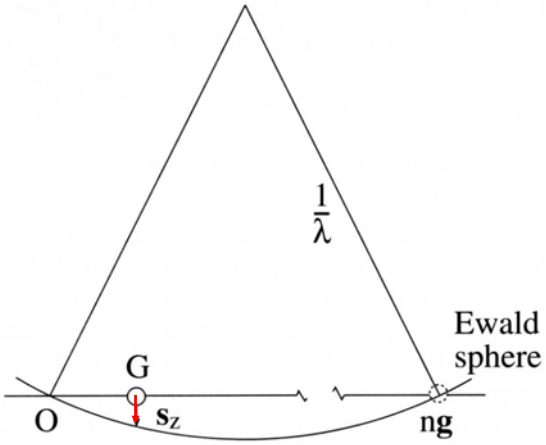


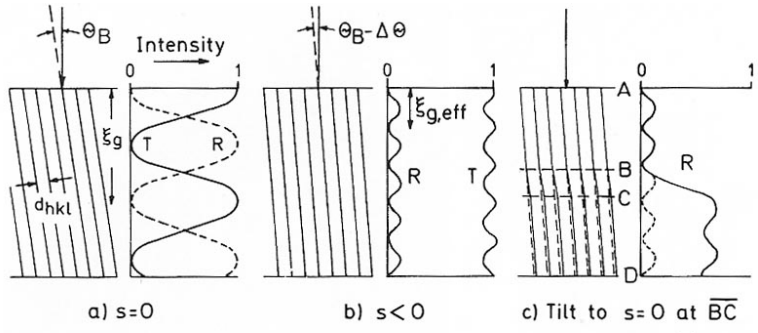
Figure 25.26. (A) Intensity contours from a simulated image of a particle like that shown schematically in (B). Notice the line of no contrast which corresponds to the plane that is not distorted by the strain field of the particle. (C) Experimental image of coherent particles in Cu-Co showing strain contrast.

LNLS
2006/2-75

Feixe Fraco – Weak Beam

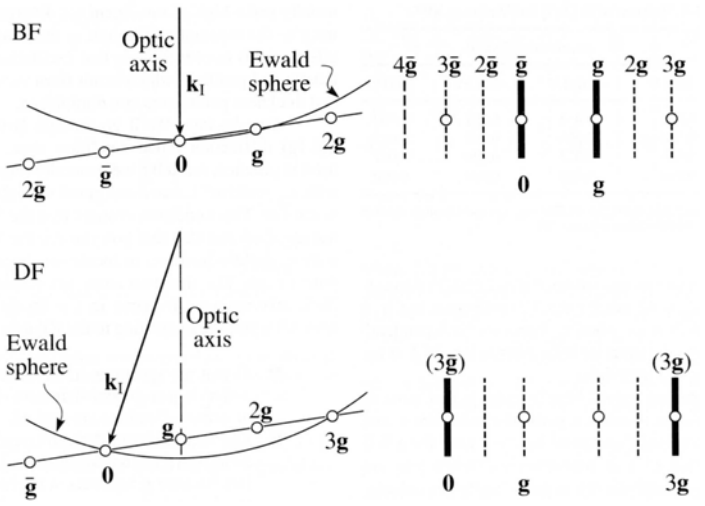


Weak Beam Dark Field



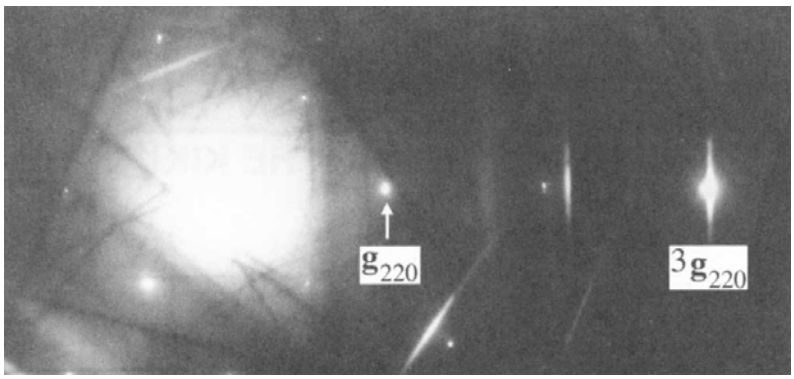
Schematic explanation of weak-beam contrast: (a) Oscillation of the transmitted T and reflected-beam intensity R in the Bragg position ($s = 0$), (b) reduction of $\xi_{g,\mathrm{eff}}$ and of the oscillation amplitudes of T and R for $s < 0$, (c) reflected intensity in the presence of a lattice-plane tilt to $s \simeq 0$ between B and C

Feixe Fraco – Weak Beam



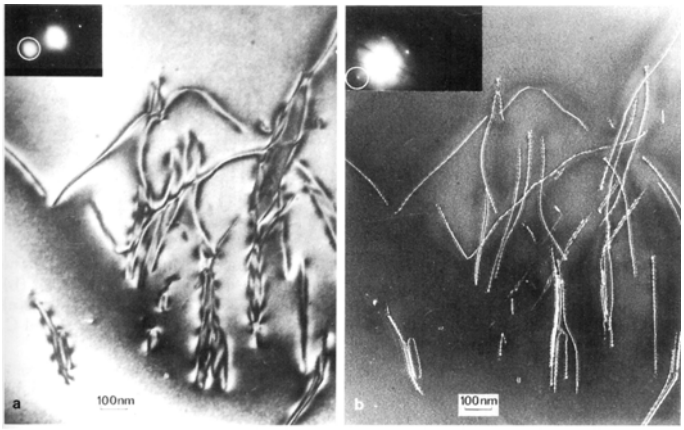
LNLS
2006/2-79

Feixe Fraco – Weak Beam



LNLS
2006/2-80

Feixe Fraco – Weak Beam



(**a**) Dislocations in heavily deformed silicon imaged with a strong $2\bar{2}0$ diffracted beam. (**b**) Weak-beam $2\bar{2}0$ dark-field image of the same area showing the increase of the resolution of dislocation detail. The insets show the diffraction conditions used to form the images [9.91]

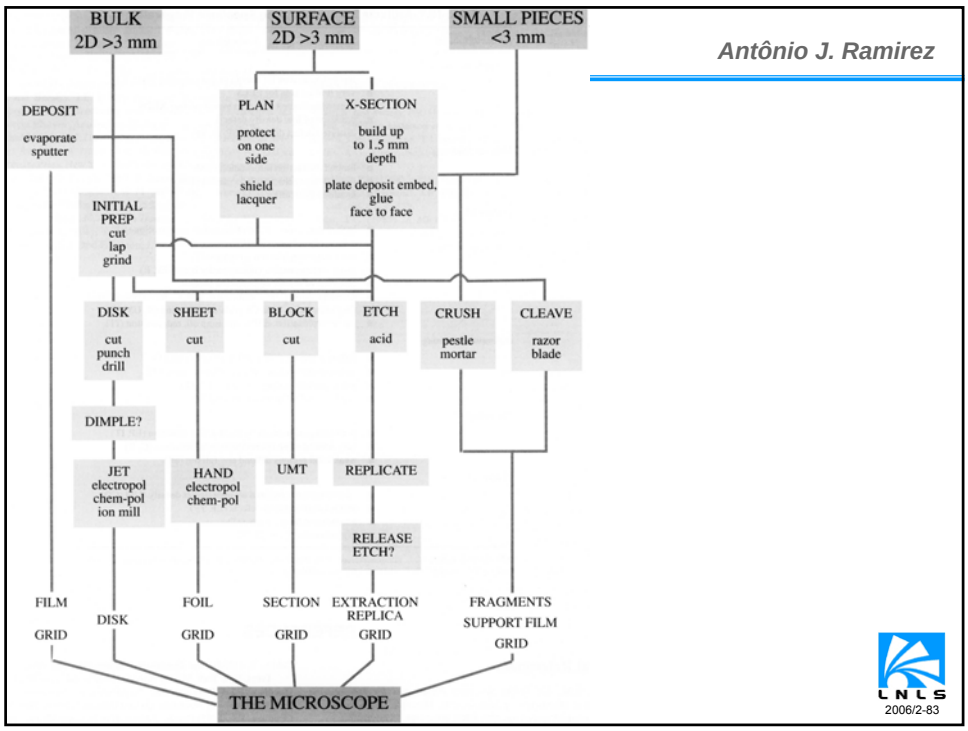
Sample Preparation

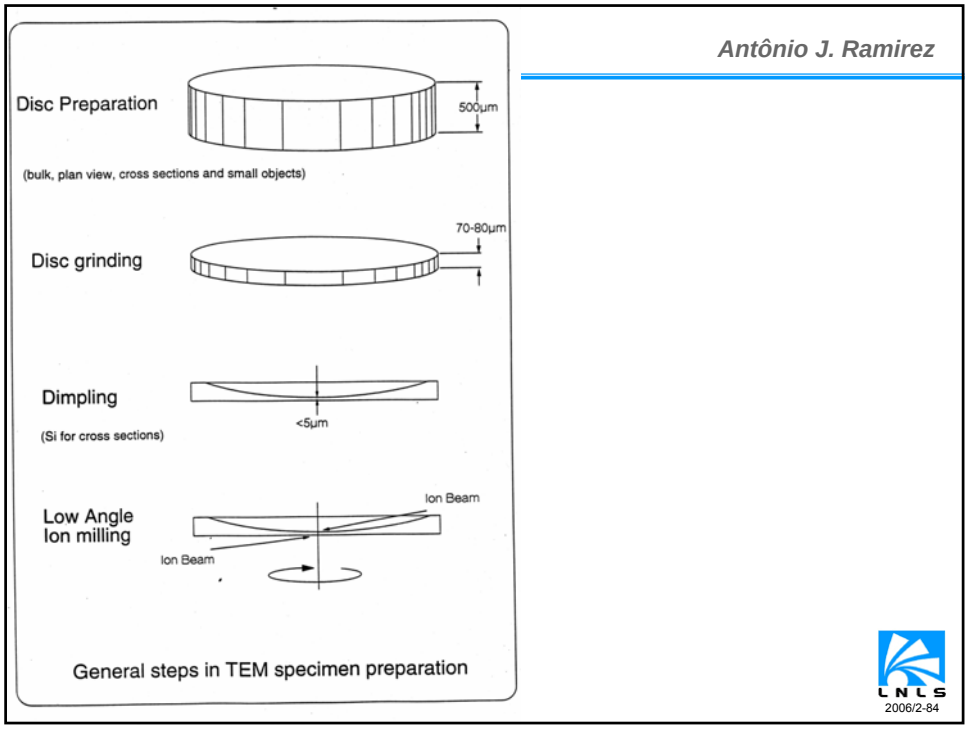
From the microscopist's point of view the ideal specimen should be:

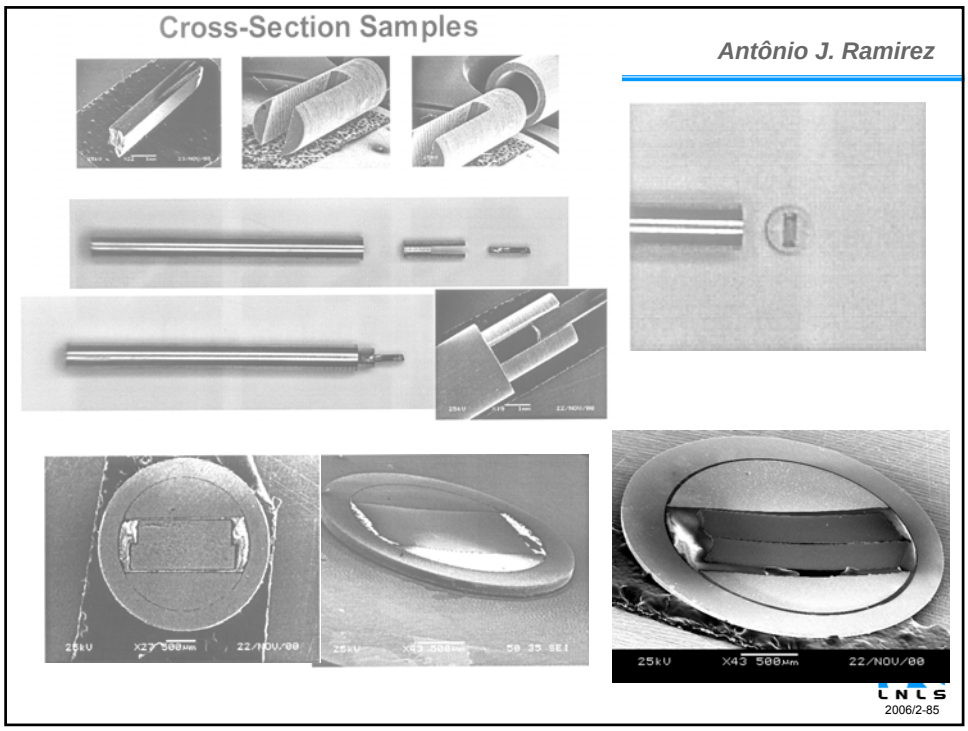
(*i*) representative; thin areas typical of bulk;
(*ii*) thin and parallel-sided over a large area;
(*iii*) largely flat

(*iv*) undamaged by preparation;
(*v*) able to be handled; not fragile;
(*vi*) stable against oxidation or other degradation;
(*vii*) free from surface segregation;
(*viii*) clean;
(*ix*) conducting; and
(*x*) non-magnetic.

Thickness: **10-50 nm (most applications)**
100 nm may be acceptable for some ones


BULK
2D >3 mm
SURFACE
2D >3 mm
SMALL PIECES
<3 mm
Antônio J. Ramirez
DEPOSIT
evaporate
sputter
PLAN
protect
on one
side
shield
lacquer
X-SECTION
build up
to 1.5 mm
depth
plate deposit embed,
glue
face to face
INITIAL
PREP
cut
lap
grind
DISK
cut
punch
drill
SHEET
cut
BLOCK
cut
ETCH
acid
CRUSH
pestle
mortar
CLEAVE
razor
blade
DIMPLE?
JET
electropol
chem-pol
ion mill
HAND
electropol
chem-pol
UMT
REPLICATE
RELEASE
ETCH?
FILM
GRID
DISK
FOIL
GRID
SECTION
GRID
EXTRACTION
REPLICA
GRID
FRAGMENTS
SUPPORT FILM
GRID
THE MICROSCOPE
LNLS
2006/2-83


Antônio J. Ramirez
Disc Preparation
500µm
(bulk, plan view, cross sections and small objects)
70-80µm
Disc grinding
Dimpling
<5µm
(Si for cross sections)
Low Angle
Ion milling
Ion Beam
Ion Beam
General steps in TEM specimen preparation
LNLS
2006/2-84


Cross-Section Samples
Antônio J. Ramirez
25kV X43 500Mm 22/NOV/00
2006/2-85